Limnol. Oceanogr., 51(2), 2006, 900–912

Bloom dynamics in early opening waters of the Arctic Ocean

Jean-Éric Tremblay[1]
Department of Biology, McGill University, 1205 Dr. Penfield, Montréal, Québec H3A 1B1, Canada

Christine Michel
Freshwater Institute, Fisheries and Oceans Canada, 501 University Crescent, Winnipeg, Manitoba R3T 2N6, Canada

Keith A. Hobson
Prairie and Northern Wildlife Research Center, Canadian Wildlife Service, Saskatoon, Saskatchewan S7N OX4, Canada

Michel Gosselin
Institut des sciences de la mer (ISMER), Université du Québec à Rimouski, 310 allée des Ursulines, Rimouski, Québec G5L 3A1, Canada

Neil M. Price
Department of Biology, McGill University, 1205 Dr. Penfield, Montréal, Québec H3A 1B1, Canada

Abstract

We measured the isotopic composition and accumulation of particulate organic matter (POM) and the uptake of carbon (C) and nitrogen (N) in an early bloom of the most productive recurring polynya of the Arctic Ocean. The estimated compensation irradiance at the onset of the bloom was similar to the average for the North Atlantic Ocean, implying that shallow mixing was of critical importance for the bloom's early initiation. Planktonic POM had a much lower $\delta^{13}C$ than ice POM, suggesting that ice-algae contributed little to the pelagic biomass. The overall isotopic fractionation of pelagic N during bloom development was consistent with in situ diatom growth under saturating irradiance and limiting NO_3^-. Soon after the ice cleared, rapid physiological changes induced an order of magnitude increase in the C and NO_3^- uptake capacity of diatoms, leading to very high *f* ratios (NO_3^- uptake : total N uptake). Most of the NO_3^- taken up appeared in the POM, so that little net release of reduced N occurred during the period of active growth. Given the tight coupling between photosynthesis and NO_3^- uptake under N limitation, the magnitude of primary production in the Arctic Ocean is expected to respond to changes in N supply.

In much of the Arctic Ocean the polar night and ice cover impose severe constraints on phytoplankton production. The duration of the production period is sensitive to climate and the extent, thickness, and seasonal melt dynamics of sea ice (e.g., Fortier et al. 2002; Laxon et al. 2003), but processes that control the timing and magnitude of organic matter production are poorly understood. Because the boreal climate is highly dynamic and susceptible to change (ACIA 2005), the question naturally arises how environmental forcing affects productivity and biogeochemical cycling in pelagic Arctic ecosystems. How early can a bloom begin after the polar night? What controls the rate and the overall yield of primary production? Answers to these questions are required to predict the large-scale consequences of changing ice cover in the Arctic Ocean. In this regard, much can be learned from present-day singularities in ice cover, such as polynyas, where open water or anomalously thin ice is surrounded by seasonally consolidated ice.

In the largest (~80,000 km^2) recurring polynya of the western Arctic Ocean, the North Water (Fig. 1), open waters can be found in late March, roughly 3 months before the onset of summer melt in adjacent regions. This condition arises from northerly winds that blow ice away from an ice arch that forms seasonally in Kane Basin and is favored by the advection of relatively warm waters in the east of the polynya (Melling et al. 2001). To our knowledge, the North Water sustains the earliest, most intense and long-lived diatom bloom north of 77°N (Klein et al. 2002; Tremblay et al. 2002*a*). Composite time series (1997–1999) showed that ~80% and 45% of the annual new and total primary pro-

[1] Corresponding author (jean-eric.tremblay@bio.ulaval.ca). Present address: Département de biologie, Université Laval, Québec, Québec G1K 7P4, Canada.

Acknowledgments

We thank Louis Fortier and the chief scientists, captains, and crews of the CCGS Pierre Esprit Radisson (Canadian Coast Guard) for invaluable support in the field. We are indebted to B. Klein for field logistics, C. Nozais and M.-È. Garneau for help in the field and laboratory, C. D. Payne for nutrient analyses, L. Harris for assistance with the mass spectrometer, and P. J. Minnett for access to PAR data. We thank Mélanie Simard for comments on the penultimate draft and anonymous reviewers for constructive comments and suggestions.

This work was funded by the Natural Sciences and Engineering Research Council (NSERC) of Canada and is a contribution to the NOW Research Network (International North Water Polynya Study) and the program of Québec Océan. Figures 1 and 2 were produced with the Ocean-Data-View Software (R. Schlitzer; http://www.awi-bremerhaven.de/GEO/ODV).

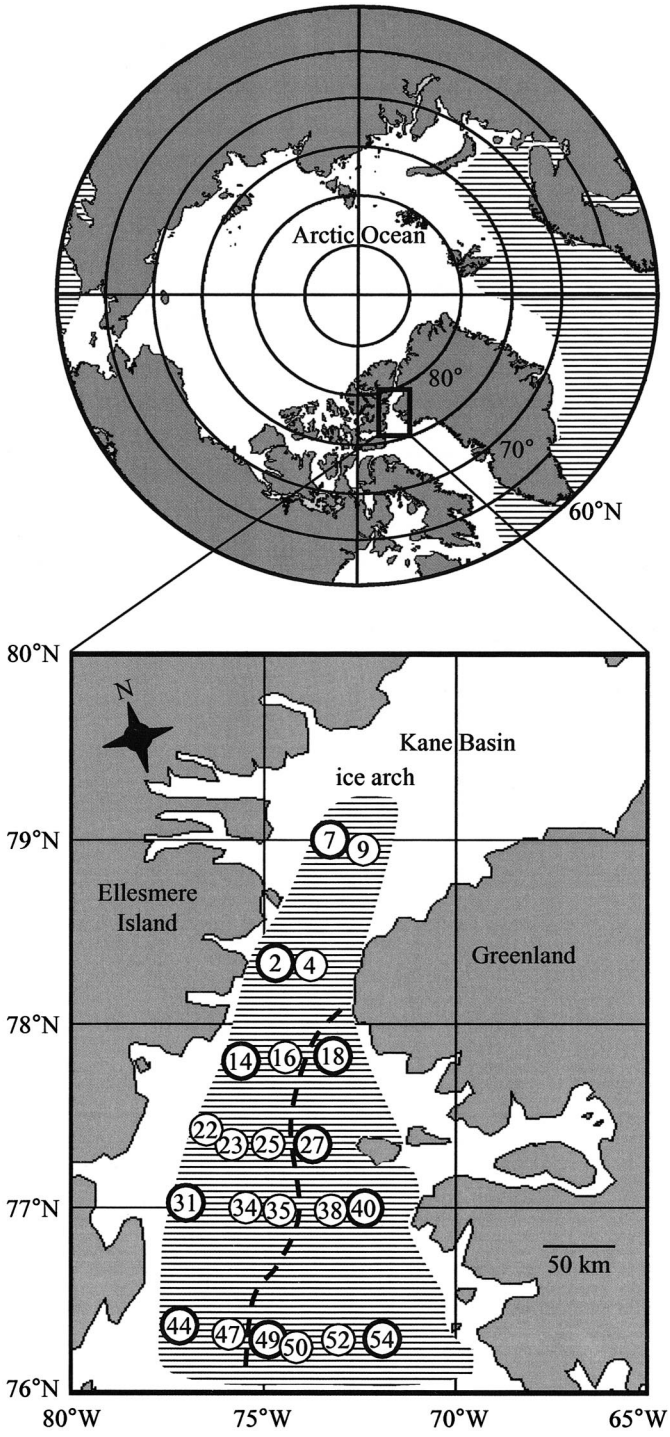

Fig. 1. Maps of the Arctic Ocean and the North Water showing the schematic extent of sea ice (white areas) and open water (hatched areas) during early May and the sampling stations for NO_3^- measurements (all circles) and phytoplankton incubations (thick circles) in Baffin Bay Water (Greenland sector) and in orthosilicic acid-rich Arctic Water (along Ellesmere Island). The dashed line indicates the mean boundary between the two water masses.

duction, respectively, occurs during the main diatom bloom (Klein et al. 2002; Tremblay and Smith 2005).

Explanations for the initiation of pelagic blooms in the Arctic generally invoke positive effects of increasing light on phytoplankton growth following the partial or complete melting of ice, or snow, or both (Niebauer 1991; Fortier et al. 2002), but the ensuing increase in surface temperature may confound interpretations. In addition, the concomitant release of ice algae can contribute substantially to the biomass of the water column (Michel et al. 1996), potentially masking causal relationships between the timing of planktonic growth and physico-chemical properties of the water. Taxonomic analysis helps to resolve this situation, but several groups of microalgae, including pennate diatoms, can grow well in both pelagic and ice environments. A parallel approach is to assess the contribution of ice algae by examining the stable isotopic signature of suspended particulate matter. Significant inputs of ice-grown algae to suspended planktonic biomass can be discerned by their relatively high $\delta^{13}C$, which presumably reflects the low availability of dissolved inorganic carbon (C) in aging ice (Kennedy et al. 1992). Additional clues into the growth conditions of microalgae can be obtained from the $\delta^{15}N$ content of organic matter (e.g., Needoba and Harrison 2004).

Recent studies indicate that the C yield of polar blooms per unit of macronutrients consumed may depart from classical Redfield stoichiometry depending on the taxonomic composition of the algal community (Arrigo et al. 1999). The C : N stoichiometry of the particulate organic matter (POM) also deviates for other reasons. First, photosynthesis can be partially decoupled from nitrogen (N) assimilation due to differential responses to light and differential production of dissolved organic nitrogen (DON) and dissolved organic carbon (DOC) by phytoplankton (e.g., Smith and Harrison 1991). Second, N uptake is partly decoupled from primary production when bacterial N consumption is significant (e.g., Allen et al. 2002) or during luxury NO_3^- uptake by diatoms (Lomas and Glibert 1999). The latter mechanism is potentially important in cold, dynamic-ice environments where phytoplankton experience abrupt shifts in irradiance. The net, combined effect of the above processes on the estimation of C-based new production from *f*-ratios (defined as NO_3^- uptake : total N uptake) or the mesoscale disappearance of NO_3^- has not been assessed at the time scale of an Arctic bloom.

We investigated the role of temperature, light, and nutrients in determining N uptake and bloom development in the North Water. Short-term incubations were used to assess the relationships between environmental variables, N uptake, and the coupling of C and N during uptake and POM synthesis. A simple budget was established from mesoscale changes in the inventories of NO_3^-, biomass, short-term N acquisition, and sinking losses. Stable isotopes of N and C were used to constrain N status and the contribution of pelagic- versus ice-grown algae to the material sampled during the bloom.

Material and methods

Data were obtained during the 1998 expedition of the International North Water Polynya Study (NOW) aboard the

Canadian ice breaker Pierre Esprit Radisson. Sampling stations were located along six east-west transects (Fig. 1) visited at least once during leg 1 (11 April–3 May), leg 2 (09–29 May), and leg 3 (4–27 June). Stas. 2, 18, 40, and 54 were revisited during leg 4 (1–21 July). The North Water was occupied by two major water masses: the fresh and orthosilicic acid-rich Arctic water (SRAW) originating from the high Arctic and the local, saline and orthosilicic acid-poor water from Baffin Bay (BBW) (Tremblay et al. 2002*b*). BBW was characterized by low northward advection (<4 cm s^{-1}; Melling et al. 2001) and its primary domain was close to Greenland, east of 74°W and south of 78°N. SRAW generally flowed with a high southward velocity (14–28 cm s^{-1}) along the coast of Ellesmere Island. The relative contribution of each water type to a given sampling site was resolved using a semiconservative tracer (Si^{ex}; Tremblay et al. 2002*b*). The time series presented here are based on stations dominated by BBW (Si^{ex} <20%) or SRAW (Si^{ex} >80%). Other stations (13 out of 32 stations) were exploited for statistical analyses only. Synoptic satellite coverage (SeaWiFs; e.g., Booth et al. 2002) indicated that bloom development and demise were synchronous throughout BBW so that all stations (18, 38, 40, 49, 50, 52 and 54) at the core of this water mass could be used to construct the time series.

Physics and macronutrients—Photosynthetically available radiation (PAR) was recorded continuously on deck using a 2 π sensor (LI-COR LI-190 SA). In the rest of the paper we refer to these measurements as incident irradiance, whereas the estimated surface irradiance, which was corrected for ice cover, is referred to as residual irradiance. Temperature, salinity, and in vivo fluorescence were recorded using a CTD (conductivity-temperature-depth instrument; Falmouth ICTD) and a Seatech fluorometer mounted on a Rosette sampler (General Oceanics Inc.). Nutrient samples were obtained from vertical profiles using 10-liter bottles (Brooke Ocean Technology Limited) attached to the Rosette. Concentrations of orthosilicic acid, soluble reactive phosphorus, $NO_3^- + NO_2^-$ and NO_2^- were determined using an ALPKEM nutrient analyzer with routine colorimetric methods (Grasshoff 1999) and an analytical detection limit of 0.05 μmol L^{-1}. During bloom development NO_2^- was nearly constant and accounted for <1% of $NO_3^- + NO_2^-$, which is hereafter designated as NO_3^-. Concentrations of NH_4^+ and urea were determined manually within 2 h of collection using the indophenol-blue (Grasshoff 1999) and diacetylmonoxine (Aminot and Kérouel 1982) methods, respectively, with analytical detection limits of 0.05 μmol L^{-1}.

Stable isotopic signatures—Samples (≥20 liters) to determine the natural abundance of ^{15}N and ^{13}C in water-column particulates were collected in the upper mixed layer (5 m). Bottom-ice samples were collected from young ice that continued to form early in the sampling period, from older floes broken off from pack ice or marginal land-fast ice. Note that the latter were not necessarily coupled spatially to sites where the water-column samples were obtained. Bottom-ice material was taken with an ice auger and melted slowly in filtered seawater. Samples were filtered onto Whatman GF/F filters using an Amicon stirred cell under gentle, constant pressure (N_2 gas), and stored frozen. Before analyses the filters were soaked in 0.1 mol L^{-1} HCl to remove inorganic C and dried. Following combustion at 1,800°C, isotopic ratios were determined with a Europa 20/20 mass spectrometer. Stable isotopic abundance is reported as a deviation (δ in ‰) from known standards:

$$\delta X = [(R_{sample}/R_{standard}) - 1] \times 1{,}000 \quad (1)$$

where X is the stable isotope and R is the corresponding $^{13}C:{}^{12}C$ or $^{15}N:{}^{14}N$ ratio. Standards were Pee Dee Belemnite for ^{13}C and atmospheric N_2 for ^{15}N. The relationship between ambient NO_3^- and the $\delta^{15}N$ of PON ($\delta^{15}N_{org}$) in the upper mixed layer was established assuming Rayleigh distillation for a closed system:

$$\delta^{15}N_{org} = \delta^{15}N_{NO_3(0)} - \{\varepsilon \times [-f/(1-f)] \times \ln f\} \quad (2)$$

where f is the fraction of unassimilated NO_3^- at sampling time (initial NO_3^- concentrations were taken from Tremblay et al. 2002*b*). Values of ε (apparent fractionation factor) and $\delta^{15}N_{NO_3(0)}$ (initial $\delta^{15}N$ of NO_3^-) are given by the slope and intercept, respectively, of the linear regression of $\delta^{15}N_{org}$ against $([-f/(1-f)] \times \ln f)$.

Nitrogen uptake and standing stocks—Samples for N uptake and the determination of particulate organic nitrogen (PON) and particulate organic carbon (POC) were taken at seven optical depths (100%, 50%, 25%, 15%, 10%, 1%, and 0.1% of incident irradiance) either at sunrise or when the sun started climbing from its lowest angle. Additional samples were collected down to 150 m for PON and POC. Given the large size of some diatoms in the North Water, all samples were screened on a 380-μm mesh to exclude the large zooplankton. Net N uptake rates were estimated using the ^{15}N labeling method under simulated in situ conditions. Duplicate 600-mL polycarbonate bottles were spiked with either $K^{15}NO_3$ or $^{15}NH_4Cl$ at 10% of ambient concentrations and incubated on deck in closed plexiglass tubes during 6, 12, and 24 h. Dual spiking with $NaH^{13}CO_3$ was performed at a subset of five stations during bloom development. The uptake of urea was estimated at a different subset of stations (27 and 40 in April, 18 in May and June, and 54 in July) throughout the entire sampling period. Temperature was maintained by pumping water from 8 m through the tubes and in situ irradiance was simulated using different combinations of optical filters. On 23 April and 3 May, uptake-irradiance relationships (*V-E*) were established simultaneously for C and NO_3^- (dual labeling) by incubating a surface sample at seven light intensities. All incubations were terminated by low-vacuum (<100 mm Hg) filtration onto precombusted 25-mm Whatman GF/F filters and copious rinsing with 0.2-μm filtered sea water. On 15 May, size-fractionation was performed onto 5-μm Nuclepore polycarbonate membranes and the filtrates were collected on GF/F filters. Inorganic C was driven off the ^{13}C-labeled filters by addition of 0.05 mol L^{-1} HCl followed by shaking for 6 h. All filters were dried at 50°C for 48 h and stored in cryovials. The ^{15}N and ^{13}C enrichment and POC and PON content of the material collected on filters were determined by mass spectrometry (Europa Scientific). Specific rates (h^{-1}) of N and C uptake were computed as follows:

$$V = (C_p - C_0)/(C_d - C_0)\Delta t \quad (3)$$

where C_p = concentration of the label (atom %) in the particulate phase after incubation, C_0 = concentration of the label (atom %) in the particulate phase at time zero, C_d = concentration of the label (atom %) in the dissolved phase at time zero, and Δt = incubation time (Collos 1987). The value of C_0 was determined from measurements of natural abundance. The range for duplicate bottles was <10% of the average. Only the averages are reported in the present paper.

Nitrogen isotope dilution was not measured because previous observations showed that it had a minimal effect on NH_4^+ uptake rates (Kristiansen et al. 1994) and *f*-ratios (Tremblay et al. 2000) in subarctic and arctic regions. The effect of incubation time on uptake was verified by fitting a linear regression to hourly uptake rates at 6, 12, and 24 h. For NO_3^-, the slope was not significantly different from zero when concentrations (ambient + tracer) were >2 μmol N L^{-1}. This result differed from previous observations in subarctic environments in which NO_3^- uptake showed marked diel changes in response to pronounced day:night cycles (Tremblay et al. 2000). In the North Water, however, such cycles were dampened by the midnight sun (24-h daylight from April onward). The mean hourly uptake of NH_4^+ was independent of incubation time at concentrations exceeding 0.2 μmol N L^{-1}. Because the apparent rates of NO_3^- and NH_4^+ uptake at 12 and 24 h were unreliable at low substrate concentrations, we used the hourly rates maintained over the first 6 h to establish the time series. The highest rate obtained at each station was referred to as V_{opt}. Unless stated otherwise, the relative contribution of NO_3^- to total N uptake was calculated as follows:

$$f\text{-ratio} = V_{NO_3}/(V_{NO_3} + V_{NH_4}) \quad (4)$$

and the relative preference index for NO_3^- as:

$$RPI_{NO_3} = f\text{-ratio}/\{(NO_3)/[(NO_3) + (NH_4)]\} \quad (5)$$

The coupling of specific C and NO_3^- uptake in the presence of photoinhibition was assessed by adjusting a double exponential relationship modified for dark uptake (Priscu 1989):

$$V = D + V_s(1 - e^{-\alpha E/V_s})e^{-\beta E/V_s} \quad (6)$$

where D = dark uptake (h^{-1}), V_s = theoretical maximum uptake in the absence of photoinhibition (h^{-1}), α = the initial slope of the *V*-*E* relationship (h^{-1} (μmol quanta m^{-2} s^{-1})$^{-1}$), E = irradiance (μmol quanta m^{-2} s^{-1}), and β = the photoinhibition parameter (the same unit as α). The observed maximum uptake in the presence of photoinhibition (V_{max}) and the photoacclimation index or irradiance at the onset of light saturation (E_K) were calculated as:

$$V_{max} = V_s[\alpha/(\alpha + \beta)][\beta/(\alpha + \beta)]^{\beta/\alpha} \quad (7)$$

$$E_K = V_{max}/\alpha \quad (8)$$

Mass balance—A budget of N during bloom development was established for the upper 100 m. This layer was chosen because significant nutrient depletion and, at times, significant suspended biomass, were observed down to 100 m (Tremblay et al. 2002*a*). Calculations required higher vertical resolution than was achieved with bottle sampling because some features of the vertical profile were not fully resolved by discrete sampling (e.g., the thickness of subsurface chlorophyll *a* [Chl *a*] maxima). To correct the inventories, station-specific relationships between PON and in vivo fluorescence were established at bottle sampling depths. These relationships were then used to interpolate PON between discrete sampling depths before vertical integration. Data on the disappearance of NO_3^- were taken from Tremblay et al. (2002*a*). Sinking losses of PON across 100 m were estimated using free-drifting sediment trap arrays (see Michel et al. 2002 for details). These losses included intact cells and debris resulting from the activity of grazers in surface waters.

Results

Bloom development and demise in BBW—Changes in physical-chemical properties and PON standing stocks were monitored in BBW (Fig. 2A–D). Surface temperatures were close to the freezing point (~−1.78°C) before May and increased very slowly until the onset of rapid atmospheric warming in early June. Likewise, salinity remained relatively constant before the establishment of melt-water stratification. Concentrations of NO_3^- were initially high and nearly uniform vertically. Net consumption began in late April, with NO_3^- decreasing progressively over the next month until it reached the detection limit in the upper 25 m. Orthosilicic acid and soluble reactive phosphorus remained in excess afterward, with mean concentrations of 2.1 ± 0.9 μmol L^{-1} and 0.5 ± 0.1 μmol L^{-1}, respectively (not shown, see Tremblay et al. 2002*b*). Concentrations of NH_4^+ were relatively low and uniform in the euphotic zone and increased to moderate values below the upper mixed layer after mid May. Standing stocks of PON remained very low until 23 April; thereafter increasing in concert with the disappearance of NO_3^- until June. High standing stocks persisted for the next 2 weeks and declined afterward.

Specific N uptake rates were plotted as a function of incubation irradiance to facilitate physiological interpretations (Fig. 2E–H). During the bloom's onset there was a transient, moderate increase in V_{NH_4} and a strong, rapid increase in V_{NO_3} at all isolumes. On nearly all occasions the V_{opt} for NO_3^- uptake occurred at intermediate irradiances. It increased 14-fold between 23 April and 3 May, leading to a net increase in maximum *f*-ratios from 0.70 to 0.96. After 3 May, V_{NO_3} decreased progressively at high irradiance. From 12 June onward V_{NH_4} was often elevated, whereas V_{NO_3} remained relatively low and stable. These changes resulted in sharply declining *f*-ratios. RPI_{NO_3} initially increased and remained close to unity until July. On 15 May, the <5-μm-size fraction accounted for 3% and 9% of the absolute uptake of NO_3^- and NH_4^+, respectively (not shown). Data on urea uptake were too scant for contouring; mean V_{urea} values in the euphotic zone were 1.1, 0.2, 0.6, and 3.4 × 10^{-3} h^{-1} for April, May, June, and July, respectively. Corresponding contributions to total N uptake were 10%, 3%, 7%, and 38%.

Seasonal progression in the northwest—Seasonal changes in temperature, NO_3^-, PON, and V_{NO_3} in the SRAW entering

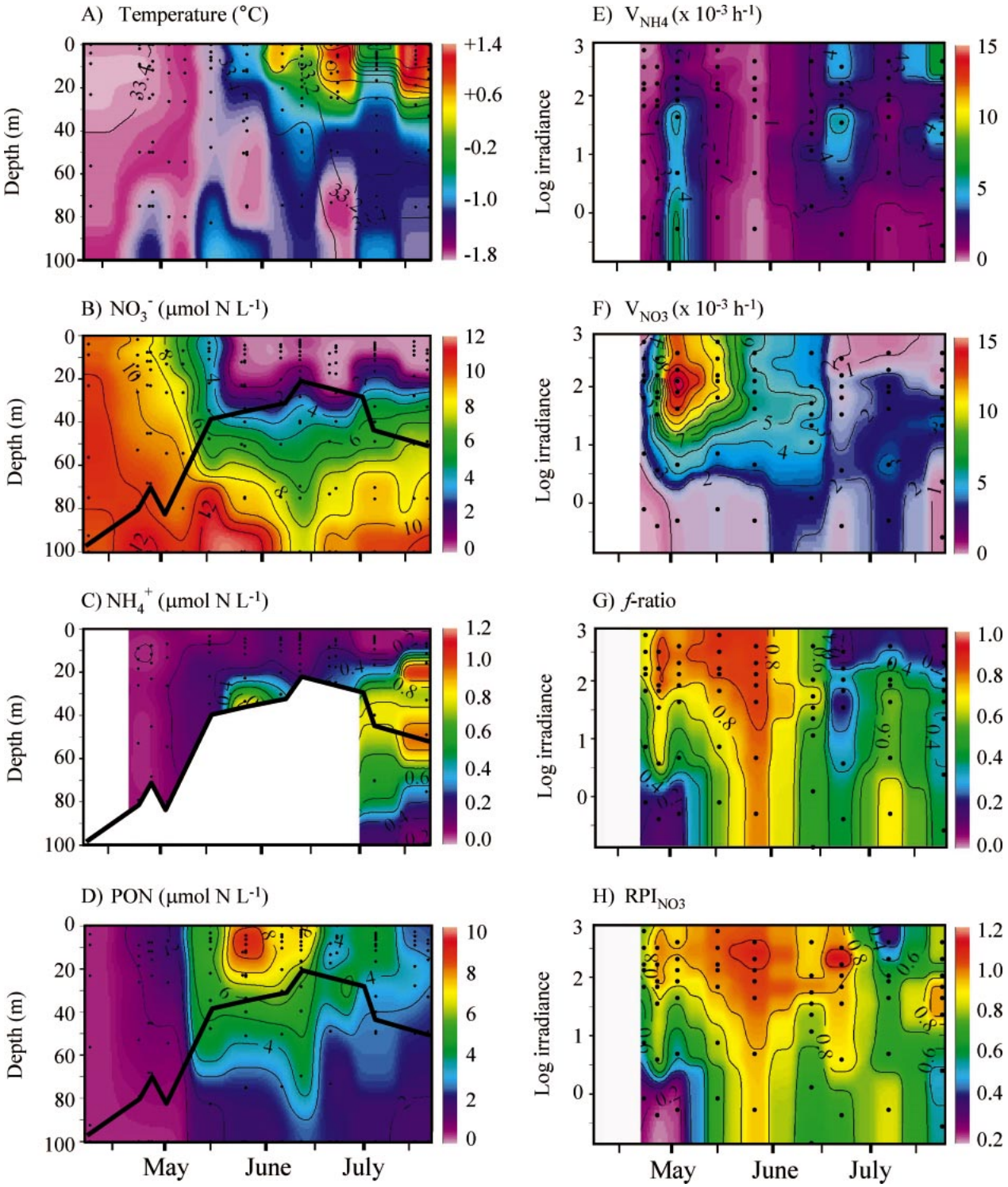

Fig. 2. Temporal changes in (A) temperature (color) and salinity (contours in ‰), (B) NO_3^-, (C) NH_4^+, (D) PON, (E) V_{NH_4}, (F) V_{NO_3}, (G) the *f*-ratio, and (H) the relative preference index for NO_3^- in BBW. Black dots mark bottle sampling depths and the thick, solid line indicates the depth of the euphotic zone. Note the change of vertical axis on the right-hand side, where the black dots correspond to those located in the euphotic zone on the left-hand side. Stations used in (A–D) are those that met the Si^{ex} criteria (see text) during legs 1 (Stas. 18, 27, 40, 49, and 54), 2 (Stas. 18, 38, 40, and 54), 3 (Stas. 18, 40, 49, 50, and 54) and 4 (Stas. 40, 54, and 58). Irradiance units are μmol quanta m^{-2} s^{-1}.

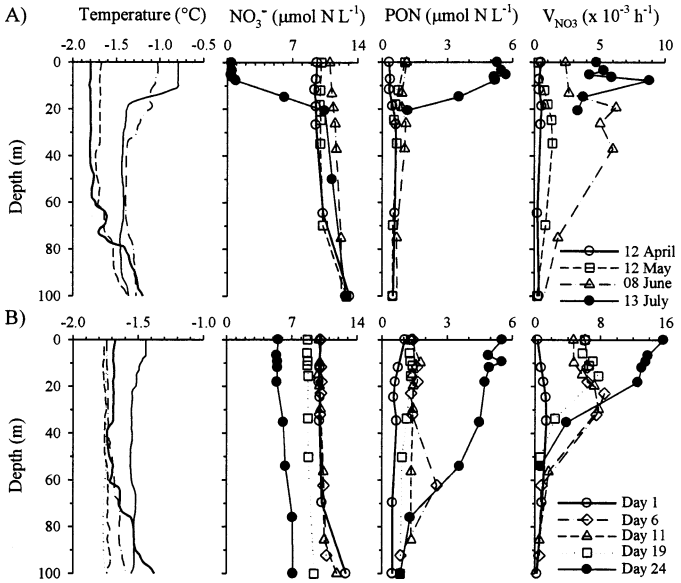

Fig. 3. Changes in temperature, NO_3^-, PON, and V_{NO_3} in pure SRAW (A) in the northwest of the survey grid (Stas. 2 and 7) from 12 April to 13 July, and (B) during the southward transit of SRAW in May. In (B), the main axis of the flow passed through Sta. 7 (Day 1), Sta. 2 (Day 6), Sta. 14 (Day 11), Sta. 31 (Day 19), and Sta. 44 (Day 24).

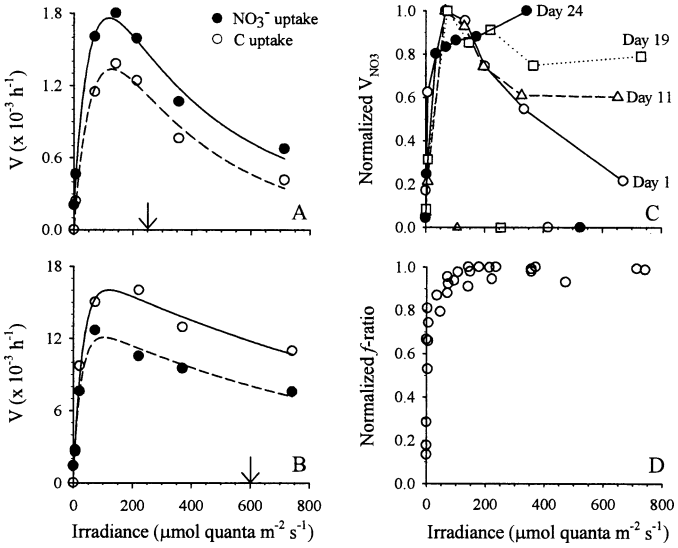

Fig. 4. Effect of incubation irradiance on (A) the specific uptake of NO_3^- and carbon on 23 April, (B) the same work on 15 May, (C) V_{NO_3} normalized to V_{opt} during the southward transit of SRAW in May, and (D) the *f* ratio normalized to the maximum observed value at each station. Arrows or symbols on the abscissa of (A–C) indicate residual irradiance.

the northeastern sector were examined (Fig. 3A). During April and May, temperature remained close to the freezing point and nearly uniform in the upper 80 m. Stratification became apparent in June and increased in July when surface temperatures reached −0.8°C. Concentrations of NO_3^- were high and almost homogenous before July, when severe depletion was observed in the upper mixed layer. This drawdown was reflected in PON standing stocks, which increased from background to moderate levels. V_{NO_3} was very low during April and May, increasing to moderate values in the nutricline during June and July.

Bloom development within southward-flowing SRAW—Stations with pure SRAW characteristics were found at all latitudes during May, making it possible to track changes in properties along the main axis of flow north to south (Stas. 7, 2, 14, 31, and 44). A mean current velocity of 14 cm s^{-1} was used to convert latitude into cumulative time the SRAW spent in the polynya (Tremblay et al. 2002*a*). The temperature remained close to the freezing point during the first 19 d and showed a modest increase on Day 24 (Fig. 3B). Concentrations of NO_3^- did not change appreciably during the first 11 d, but decreased slightly by Day 19 and moderately by Day 24. This decline was mirrored by a corresponding increase in PON. V_{NO_3} was initially very low and increased to moderate values on Days 11–19 and to very high levels on Day 24.

Irradiance-dependence of photosynthesis, NO_3^- uptake and f-ratios—The most salient features of the *V-E* curves in BBW were the increase in V_{max} and the loss of photoinhibition between 23 April (Fig. 4A) and 15 May (Fig. 4B). In contrast, the photoacclimation index (E_K) showed a nonsignificant, decreasing trend (Table 1). Photosynthesis and V_{NO_3} were strongly coupled because their E_K values and relative photoinhibition were coherent, and dark NO_3^- uptake accounted for a very small fraction of V_{max}. *V-E* experiments were not performed in SRAW, but the deck incubations with $^{15}NO_3^-$ are an acceptable substitute at stations with high (>5 μmol N L^{-1}) and vertically uniform NO_3^- during the southward transit in May (see Fig. 3B). For ease of comparison among sites, V_{NO_3} was normalized to V_{opt} and plotted against incubation irradiance (Fig. 4C). Complete recovery from se-

Table 1. Values ± standard deviations of uptake-irradiance parameters for C and NO_3^- on 23 April and 15 May 1998 in the BBW sector of the North Water.*

Date	Label	*D*	V_{max}	α	β	E_K
23 Apr	NO_3^-	0.19±0.08	2.42±0.34	0.042±0.009	0.006±0.002	37±10
	C		2.18±0.34	0.033±0.005	0.006±0.002	40±9
15 May	NO_3^-	0.47±0.90	13.1±1.4	0.471±0.132	0.012±0.005	25±7
	C		17.8±1.3	0.573±0.075	0.012±0.004	28±4

* Units are 10^{-3} h^{-1} for *D* (dark NO_3^- uptake) and V_{max} (maximum uptake in the presence of photoinhibition), 10^{-3} h^{-1} (μmol quanta m^{-2} s^{-1})$^{-1}$ for α (initial slope) and β (photoinhibition parameter), and μmol quanta m^{-2} s^{-1} for E_k (photoacclimation index).

vere photoinhibition was achieved during the 24 days of transit. The irradiance at V_{opt} remained invariant during the first 19 d and systematically lower than residual irradiance at surface. A conservative E_K estimate of ~30 μmol quanta m^{-2} d^{-1} was deduced for this period. The effect of irradiance on *f*-ratios in BBW and SRAW was assessed by normalizing discrete *f*-ratios to the maximum value at each high NO_3^- station. The *f*-ratio increased rapidly with irradiance up to 100 μmol quanta m^{-2} d^{-1} and remained nearly constant above this threshold (Fig. 4D).

Concentration dependence of N uptake and f-ratios—The effect of ambient nutrients on N uptake after midbloom (i.e., NO_3^- <8.0 μmol L^{-1}) were examined using all incubations at irradiances higher than or equal to that at V_{opt} (uptake was otherwise light-limited). First-order changes in V_{NO_3} were consistent with Michaelis-Menten kinetics in BBW (r^2 = 0.95) and SRAW (r^2 = 0.89), but the latter showed a high V_{max} (0.018 ± 0.001 h^{-1}) and low K_s (1.1 ± 0.2 μmol N L^{-1}) relative to BBW (V_{max} = 0.015 ± 0.3 h^{-1}; K_s = 1.9 ± 0.3 μmol N L^{-1}) (Fig. 5A). The specific uptake of reduced N was positively related to ambient concentrations in the two water masses, but did not reach saturation at the low concentrations observed (Fig. 5B). The affinity of uptake (i.e., initial slope of the relationship) was steeper for urea (0.033 ± 0.002 h^{-1}[μmol N L^{-1}]$^{-1}$) than for NH_4^+ (0.010 ± 0.002 h^{-1}[μmol N L^{-1}]$^{-1}$). For comparison, the initial slopes for V_{NO_3} (NO_3^- < 1 μmol N L^{-1}) were 0.005 and 0.009 in BBW and SRAW, respectively. The *f*-ratio was linearly related to NO_3^- at concentrations <0.6 μmol N L^{-1} (r^2 = 0.80), remaining high and relatively invariant above this threshold (Fig. 5C). No second-order effects of temperature, irradiance, or NH_4^+ were detected in the residuals of Fig. 5A and C (insert) or from multiple regressions of log-transformed data.

N budget and C : N coupling—Mass balance in BBW was established by comparing the nitrate deficit with the accumulation of PON in the upper 100 m and the sinking flux of PON across 100 m. The sinking flux of PON was low at the beginning and end of the sampling period, with maximum values at the peak of the bloom (Fig. 6A). Cumulative sinking at the time points at which data on nitrate deficit and suspended PON were available was calculated by interpolation and trapezoidal integration. Considering all BBW stations, regression analysis (major reduced axis) indicates that 73% of the NO_3^- consumed by 12 June (peak of the bloom) accumulated into PON, 19% was lost to sinking, and the remaining 8% was unaccounted for (Fig. 6B).

Relative changes in net NO_3^- uptake and primary production (slope = 7.5 ± 0.3 mol : mol, r^2 = 0.92) and the concomitant assimilation of C and N into POM (slope = 6.4 ± 0.1 mol : mol, r^2 = 0.98) were tightly coupled at NO_3^- concentrations >2.0 μmol N L^{-1} (Fig. 6C).

Stable isotopes—The isotopic signatures of pelagic PON were investigated in relation to those of bottom-ice material. During the bloom, the fraction of unassimilated NO_3^- at the surface explained 84% of the variance in pelagic $\delta^{15}N_{org}$, with an apparent isotopic fractionation factor (ε) of 5.7 ±

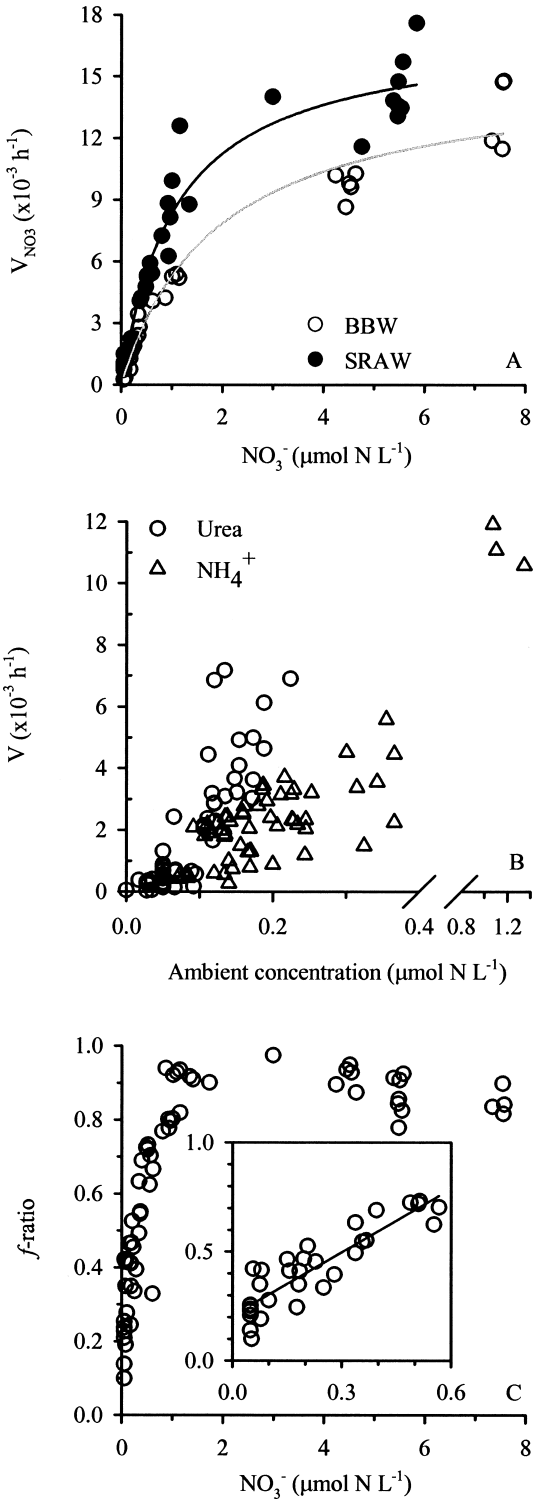

Fig. 5. Relationships between ambient N concentrations and (A) V_{NO_3} in BBW and SRAW fitted with the Michaelis-Menten model $V = V_{max} + S/(K_s + S)$ where V_{max} is the uptake rate at saturation, S is the NO_3^- concentration and K_s the half-saturation constant, (B) V_{NH_4} and V_{urea} at all stations, and (C) the *f*-ratio over the entire range of NO_3^- concentrations and at concentrations <0.6 μmol N L^{-1} (insert).

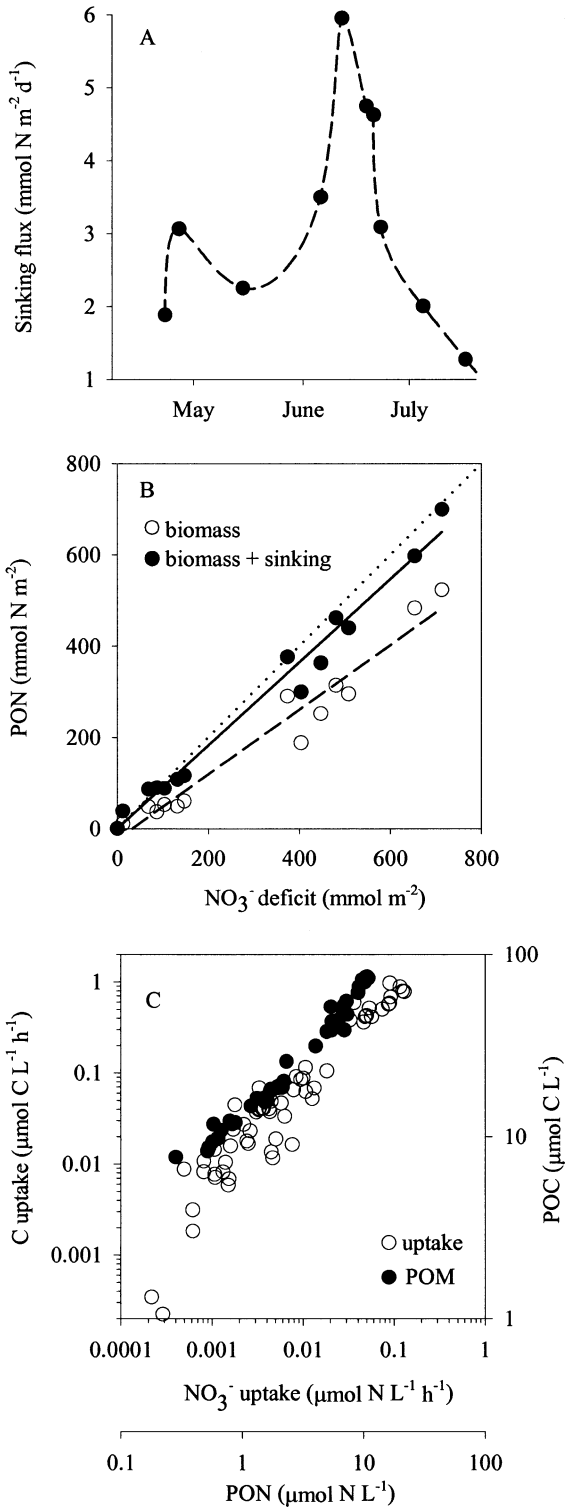

Fig. 6. (A) Sinking flux of PON at 100 m and relationships between (B) NO_3^--deficit and PON with (closed circles and solid line) and without (open circles and dashed line) the addition of cumulative sinking losses (the dotted 1 : 1 line is shown for visual reference), (C) C and N during uptake and POM synthesis.

0.5‰ (Fig. 7A). It follows that pelagic samples taken early in the bloom were the most depleted in ^{15}N. Figure 7B shows that these samples were the most depleted in ^{13}C, and also those whose dual isotopic signature overlapped with some bottom-ice samples (Fig. 7B). The overlapping samples were from thin ice, as indicated by the strong positive relationship between ice thickness and bottom-ice $\delta^{13}C_{org}$ (Fig. 7C). Bottom-ice samples for which coupled measurements of $\delta^{13}C_{org}$ and Chl *a* were available are presented in Table 2. The concomitant temporal increase in $\delta^{13}C_{org}$, Chl *a* inventory, and ice thickness showed that only the newly formed ice with low Chl *a* had isotopic overlap with the pelagic bloom.

Discussion

Temporal analysis of the stable isotopic and taxonomic composition of the bloom showed that release of ice algae did not significantly contribute to changes in the biological characteristics of the water column. From the onset to the peak of the bloom, at least 85% of the planktonic, microalgal biomass was found in chain-forming (*Thalassiosira* spp.) and very large, solitary (*Actinocyclus* sp. and *Coscinodiscus* sp.), centric diatoms that thrive in the pelagic environment (Lovejoy et al. 2002). The ribbon-shaped, pennate diatoms *Fossula Arctica* and *Fragilariopsis* sp., which were present in low numbers in the plankton throughout April and May (Lovejoy et al. 2002), were the dominant species at the bottom surface of thin and moderately thick ice, respectively (Simard 2003). This observation suggests that some pelagic algae were included in young ice, thus contributing to the isotopic overlap between the two biota (Fig. 7A). Thicker ice with high Chl *a* biomass was observed after the peak of the bloom (Table 2) and was numerically dominated by *Nitzschia frigida* (Simard 2003). The contribution of this pennate diatom to pelagic biomass was systematically negligible at our sampling sites (Lovejoy et al. 2002).

In situ growth of the pelagic bloom was substantiated by the well-documented relationship between the fraction of unassimilated NO_3^- and the $\delta^{15}N$ of PON (Fig. 7B) (e.g., Needoba et al. 2003). The intercept of the regression line in Fig. 7A implies an initial $\delta^{15}NO_3^-$ of 8.4 ± 0.2‰, which agrees with direct measurements in surface waters of the subarctic Pacific (8.3 ± 0.1‰; Wu et al. 1997) containing similar concentrations of nitrate. To our knowledge, no direct measurements of $\delta^{15}NO_3^-$ were performed in Baffin Bay, but the $\delta^{15}N_{org}$ of fresh sediment underlying nitrate-depleted waters of the high Arctic implies $\delta^{15}NO_3^-$ values ranging from 8.3 to 10.7‰ (Schubert et al. 2001). Relatively high $\delta^{15}NO_3^-$ can be caused by pelagic denitrification (Ganeshram et al. 1995), but the latter is unlikely in the well-oxygenated waters of the Arctic Ocean. Although sediment denitrification is substantial on Arctic shelves it apparently imparts little isotopic fractionation on deep NO_3^- (Brandes and Devol 1997). Thus, we conclude that the high $\delta^{15}NO_3^-$ at surface relative to deep waters (global mean of ~5–6‰) indicates that the water column is not entirely homogenized during autumn and winter, consistent with the strong halocline that characterizes much of the Arctic Ocean.

The strong, positive relationship between $\delta^{13}C_{org}$ and the

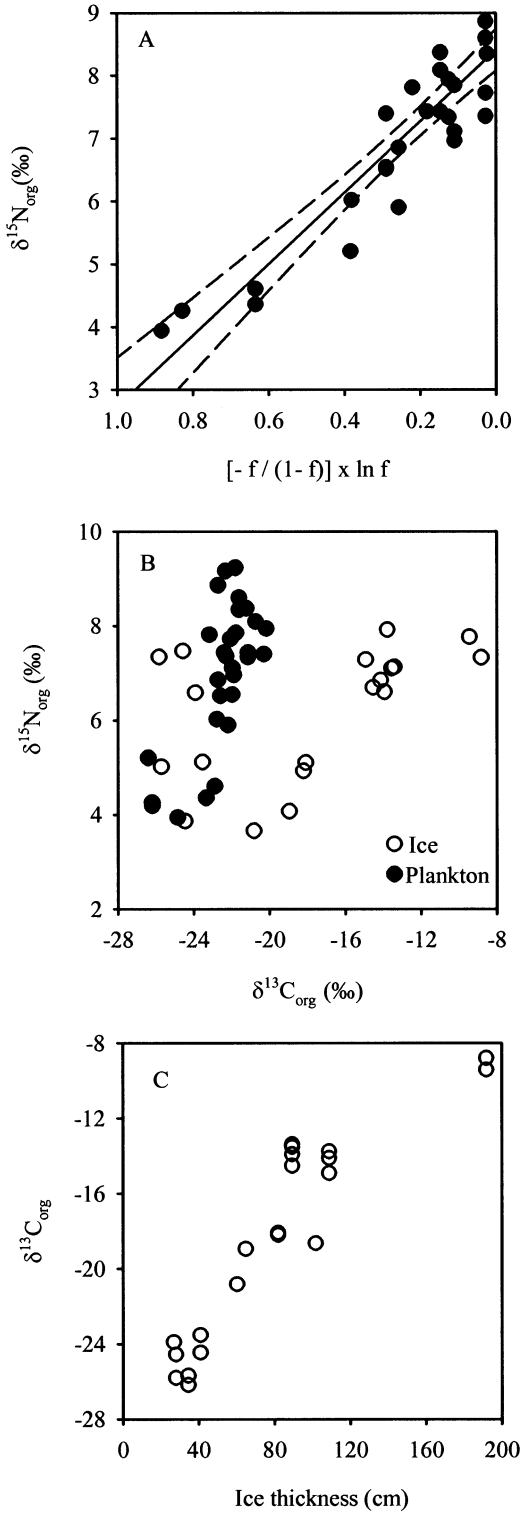

Fig. 7. Stable isotopic signature of (A) pelagic PON against the fraction of unassimilated nitrate expressed as $([-f/(1-f)] \times \ln f)$, (B) PON and POC in pelagic and bottom-ice samples, and (C) bottom-ice POC against ice thickness. Two ice stations, one associated with anomalous snow cover (60 cm vs. a mean of 5.5 cm for all other stations) and another one south of the polynya proper were excluded from analyses (not plotted).

Table 2. Ice thickness and bottom-ice Chl *a* and $\delta^{13}C_{org}$ for drifting pack ice and marginal fast ice in the North Water region during three sampling periods in spring 1998 (mean ± standard deviation).

Period	*N*	Thickness (cm)	Chl *a* (mg m^{-2})	$\delta^{13}C_{org}$ (‰)
1–15 May	4	33±7	2±1	−24.9±1.3
15–31 May	4	85±20	21±15	−16.7±3.3
1–10 June	2	182±15	63±2	−13.2±5.3

thickness of ice (Fig. 7C) was previously observed in the Ross Sea (Arrigo et al. 2003). A cohesive, boundary layer probably exists around cells under conditions of laminar flow within brine channels. More complete utilization of the inorganic C trapped in this layer relative to the bulk medium can lead to high particulate $\delta^{13}C_{org}$ (Kennedy et al. 2002). The absence of high $\delta^{13}C_{org}$ values in the water column confirms that ice-grown algae did not make quantitatively significant contributions to the developing bloom at our sampling sites. Thus the changes in N uptake and suspended PON reported herein can be legitimately linked to changes in local water-column properties.

The interpretation of water-column N dynamics requires prior assessment of the potential contribution of bacteria to absolute N uptake. Two lines of evidence show that uptake was mediated primarily by phytoplankton until at least 12 June. First, the <5-μm-size fraction accounted for only 3% and 9% of NO_3^- and NH_4^+ uptake at midbloom (15 May). Assuming that at most half of the bacteria pass though GF/F filters (Kirchman et al. 1989) would increase their potential shares to 6% and 18%. These shares are certainly overestimated because ~20% of the total Chl *a* was in the <5-μm-size fraction at this time (Mei et al. 2002). In the case of NO_3^-, the small contribution of bacteria before and during the bloom is confirmed by the ratio of dark to light-saturated uptake on 23 April (0.08) and 15 May (0.04) (Table 1). The contribution of bacteria was presumably greater during the postbloom period, but this has little bearing on our conclusions.

The early bloom in the eastern North Water at 77°N suggests peculiar physico-chemical conditions or biological adaptation or acclimation of the dominant diatoms. For example, oceanic blooms associated with the ice edge in the Barents Sea at 77°30′N (Strass and Nöthig 1996) and with ice-free waters in the North Atlantic at 75°N (Siegel et al. 2002) do not begin before late May or early June. In the seasonally ice-covered Barrow Strait, adjacent to the polynya, pelagic blooms are initiated between late July and August (C. Michel pers. comm.). There are reports of blooms beginning as early as April north of 77°N, but in contrast to the North Water these are either associated with fronts, the stabilizing influence of melting ice (Niebauer 1991), or strong dominance by *Phaeocystis* sp. (Smith et al. 1991). The diatom outburst in the North Water began roughly at the same time as the North Atlantic bloom at 55°N, where temperature and incident irradiance are ~7°C warmer and 10 times higher, respectively. At first glance, this difference suggests that diatoms were particularly well acclimated to

low temperature and low irradiance or suffered small losses in the North Water.

The onset of temporal changes in PON for BBW (Fig. 2) implies that vertical mixing was adequate for net growth around 23 April. At bloom initiation the mean depth of the mixed layer is by definition close to the critical depth (Z_{cr}) where depth-integrated gross production equals losses (Smetacek and Passow 1990). At this time, the average depth of the mixed layer was 34 m, based on the median value of 16 CTD profiles and a criterion of 0.01 for density difference (see Tremblay et al. 2002*b*). With this information, a compensation irradiance (E_c = irradiance at which gross production equals community losses) of 1.9 ± 0.3 mol quanta m^{-2} d^{-1} was obtained using values of 0.087 m^{-1} and 5.8 ± 1.0 mol quanta m^{-2} d^{-1} for the coefficient of diffuse light attenuation and the mean residual irradiance, respectively, at BBW stations during late April. Given the wide range of published E_c (0.35 to 3.5 mol quanta m^{-2} d^{-1}), our estimate is considered similar to the empirical value of 1.3 ± 0.3 mol quanta m^{-2} d^{-1} derived for the North Atlantic (35–75°N; Siegel et al. 2002) and implies that unusually high production : respiration ratios or low losses are not necessary to explain the precocious onset of the BBW bloom.

Responses of V_{NO_3} and photosynthesis to irradiance imply that cells were initially shade-acclimated (Table 1, Fig. 4A–C). During bloom development, E_K was similar to the mean residual irradiance in the upper mixed layer on 23 April (22 ± 4 mol quanta m^{-2} d^{-1}). Cells were thus acclimated to the under-ice light climate but not to the higher irradiance found in the more open waters. In the following weeks, E_K remained low and typical of diverse phytoplankton assemblages in polar regions and the North Atlantic (Harrison and Platt 1986). Due to declining and eventually limiting NO_3^- concentrations after 15 May it would have been difficult to interpret changes in E_K as the sole result of photoacclimation. However, the relatively high E_K (132–500 μmol quanta m^{-2} s^{-1} compared to <40 μmol quanta m^{-2} s^{-1} in our Table 1) obtained during late summer (Kashino et al. 2002) confirms that the cells were acclimated to low irradiance throughout the onset of the bloom.

The similarity of apparent compensation irradiances of the phytoplankton between the North Water and the North Atlantic shows that shallow mixing or neutral buoyancy was instrumental in the precocious BBW bloom. Processes responsible for the maintenance of shallow mixed layers are detailed elsewhere (Melling et al. 2001; Tremblay et al. 2002*b*). The current view is that upwelling or upward mixing of the heat supplied by the West Greenland Current in April was not sufficient to induce net warming and outright ice melting, but impeded cooling and ice growth (Melling et al. 2001). In essence, the early bloom in the BBW sector of the North Water was linked to the favorable light regime imparted by mechanical ablation of the ice cover and buoyancy-restoring forces. This situation departs from the ''classical'' ice-edge scenario in that net growth began more than a month before ice melt stratification.

Three lines of evidence show that the availability of light did not have a strong influence on the initial rate of bloom development. First, the increase in V_{NO_3} from 23 April to 3 May occurred at all isolumes (Fig. 2F), implying widespread, physiological changes in uptake capacity. Second, V_{NO_3} was initially strongly inhibited upon exposure to mean irradiances exceeding 100 mol quanta m^{-2} s^{-1} (Fig. 4A–C). The severity of photoinhibition progressively decreased with time in BBW and along the axis of SRAW flow, implying an increasing ability of the phytoplankton to harvest the relatively high light associated with open waters. Finally, the overall, apparent isotopic fractionation factor ε = 5.7 ± 0.5‰ during the bloom (Fig. 7B) was consistent with published values for the genus *Thalassiosira* (i.e., the dominant genus of the bloom) grown on high NO_3^- and saturating irradiance (6.3 ± 0.4‰; Needoba et al. 2003). Although we assumed a closed system and fitted a single line to the data in Fig. 7A, it should be noted that the increase in $\delta^{15}N$ was initially modest. This small deviation from linearity suggests that the ''closed system'' assumption was not entirely valid during May due to episodic replenishment of NO_3^- in the euphotic zone (Tremblay et al. 2002*a*).

The coupling of photosynthesis and NO_3^- uptake shows that initial increases in V_{opt} and f ratios at all light intensities were driven by proportional increases in the electron harvest capacity of dominant diatoms. In shade-acclimated cells, the dark reactions of photosynthesis are initially slow due to the low turnover of photosystem II traps (τ) and reduced inventories of photosynthetic units and enzymes (Richardson et al. 1983). The probability of encounter between a photon and a closed trap is high and the excess energy is dissipated as heat (nonphotochemical quenching; NPQ) and fluorescence, consistent with severe photoinhibition in late April (Fig. 4A,B). Upon exposure to high irradiance, shade-acclimated cells typically show an increase in τ and the amount of enzymes per electron transport chain. In the North Water, increases in V_{opt} were synchronized with the loss of photoinhibition despite relatively constant E_K. Such decoupling suggests that changes in the dark reactions of photosynthesis preceded seasonal acclimation of the light reactions.

The combination of minimal photoacclimation and rapidly increasing V_{opt} suggests a significant role of water temperature because it affects only the dark reactions of photosynthesis. This mechanism may have played a role in the northwest (Fig. 3A). In BBW, however, the rise to maximum V_{NO_3} was accompanied by a minute temperature increment (0.1°C; Fig. 2A). This small change could not cause a 14-fold increase in V_{opt} because the implied Q_{10} would have to be orders of magnitude higher than established values for NO_3^- uptake in polar phytoplankton (Smith and Harrison 1991). However, the internal temperature of diatoms could have been higher than ambient due to NPQ. Some authors attribute significant warming and stratification of the water column to phytoplankton at moderate Chl *a* concentrations (Dickey et al. 2001; Mei et al. 2002). If this heat can sway the thermal inertia of a large volume of water it should have a stronger, immediate effect on internal cellular temperature.

Direct stimulation of enzymatic activity by thermal dissipation would explain the results only partly because even if internal temperatures reached the optimum for NO_3^- reductase (e.g., 15°C for the polar species *Thalassiosira antarctica*; Gao et al. 2000), the change in V_{opt} would be only half the observed increase. Notwithstanding, the results show that the initial increase in V_{opt} was a cellular response

of the pelagic diatoms that lead to a greater capacity for electron transport and POM synthesis independently of ambient temperature. Potentially stimulating effects of rising ambient temperatures on V_{NO_3} after mid-May in BBW would have been obscured by the detrimental effect of decreasing N concentrations on growth rates. The requirements of diatoms for NO_3^- were high in the North Water because their apparent K_s (Fig. 5A) were within range of the maximum values reported for the Barents Sea (1.8–2.2 μmol N L^{-1}; Kristiansen and Farbrot 1991; Kristiansen et al. 1994), the Greenland Sea (2.24 μmol N L^{-1}; Muggli and Smith 1993) and the Canadian Archipelago (0.87 μmol N L^{-1}; Smith and Harrison 1991). Thus the case cannot be made for a first-order effect of ambient temperature on NO_3^- acquisition and diatom growth in the North Water. The initial stimulation of enzyme synthesis by heat dissipation is a plausible mechanism, but one that we cannot distinguish from an endogenous response to elevated irradiance.

The decline in V_{NO_3} after mid-May was not related to changes in the concentration of NH_4^+ in BBW (Fig. 2), implying that NH_4^+ did not inhibit the uptake of NO_3^-. This observation contrasts with previous reports of inhibition in the Arctic (Smith and Harrison 1991) and is presumably explained by the persistently low concentrations of NH_4^+ in the upper euphotic zone of the North Water. In this context, it must be the combination of vanishing NO_3^- at the surface and the relatively strong affinity of uptake for NH_4^+ and urea in BBW (Fig. 5B) that led to declining *f*-ratios (Figs. 2 and 5C) and N dynamics typical of postbloom, recycling communities in surface waters. Moderate RPI_{NO_3}, V_{NO_3}, and *f*-ratios in the nitracline were associated with a persistent layer of the centric diatom *Chaetoceros socialis*, which drove most of the residual new production after the early bloom. The high affinity of urea uptake relative to other N sources in our study is difficult to explain, but consistent with previous work elsewhere (e.g., Cochlan and Bronk 2001).

Net diatom growth in the North Water was fueled by NO_3^- due to low initial inventories of NH_4^+ (Fig. 2) and urea (Fig. 5B). However, the significance of NO_3^- uptake for new production depends on the extent of assimilation into PON. In polar waters, decoupling can be caused by the release of fresh DON by phytoplankton, especially at high irradiance (e.g., Hu and Smith 1998). Incomplete assimilation of the NO_3^- taken up (i.e., luxury uptake) by diatoms at low temperature potentially results in the release of NO_2^-, NH_4^+, or DON. According to a recent hypothesis, this ''futile'' reduction of NO_3^- would serve as an electron sink to attenuate the stress caused by transient exposure to high irradiance (Lomas and Glibert 1999). The high initial RPI_{NO_3} in BBW (Fig. 2H) could be construed as an indication of luxury NO_3^- uptake, but saturating V_{NO_3} kinetics (Fig. 5A), coupled C-NO_3^- uptake (Figs. 4A,B and 6C) and the nearly constant RPI_{NO_3} at irradiances >100 μmol quanta m^{-2} s^{-1} suggest that excess light did not induce luxury uptake of NO_3^-. Also, the nearly invariant concentrations of NO_2^- (see Material and Methods) and NH_4^+ (Fig. 2C) in the upper euphotic zone imply that inorganic N released by the cells, if any, must have been readily reassimilated. This notion is supported by changes in the $\delta^{15}N$ of PON during the bloom (Fig. 7A). In this context, the mass balance exercise in Fig. 6B implies that, at the very most, 8% of the NO_3^- taken up was transferred to DON.

The cumulative *f*-ratios were calculated after separate vertical and temporal integration of absolute rates for each N source. This integration was performed previously for NO_3^- uptake and yielded a cumulative uptake nearly identical to that based on the mesoscale disappearance of NO_3^- in BBW (Tremblay et al. 2002*a*). The concordance may seem surprising because the in vitro uptake rates were not corrected for ice cover and did not account for consumption by ice algae. However, the bulk of NO_3^- uptake occurred under minimal or no ice cover (Tremblay et al. 2002*a*). At the end of the bloom the cumulative *f*-ratio was 0.69 (0.65 when urea was included in calculations; not shown), indicating that a large portion of total primary production was available for export to higher trophic levels and the deep waters (Eppley and Peterson 1979). The average and the range of *f*-ratios at individual stations were similar to those obtained in the Northeast Water polynya (Smith et al. 1997), but much higher than those measured during summer in adjacent Baffin Bay after ice breakup (Harrison et al. 1982).

The overall *f*-ratio was not significantly biased by isotopic dilution of the $^{15}NH_4$ label during incubations. First, the nearly constant concentrations of NH_4^+ in the upper euphotic zone implied that regeneration was balanced by uptake in situ (Fig. 2C, E). A numerical simulation initialized with ambient concentrations and apparent uptake rates indicates that the dilution bias of uptake rates was negligible, especially because the large zooplankton that contribute to NH_4^+ excretion were absent from incubation bottles. At concentrations <0.2 μmol N L^{-1}, substrate depletion (i.e., negative slopes of normalized uptake against time, see Material and Methods) was a potentially more serious bias, but one that was limited by considering short incubations only. Independent validation of the cumulative in vitro *f*-ratio at the peak of the bloom (*f*-ratio = 0.85 on 25 May) is provided by dividing the slope of POC against PON by the slope of C versus NO_3^- uptake in Fig. 6C (*f*-ratio = 0.85; which is independent of experimental estimates of NH_4^+ uptake). At concentrations >0.2 μmol N L^{-1}, the apparent hourly uptake rates were independent of incubation time (see Material and Methods) despite the expectation that isotopic dilution should increase with incubation time. The bias potentially became important during mid-July when NH_4^+ accumulated in the lower euphotic zone, but its impact on the cumulative *f*-ratio and our conclusions would be minimal.

Summary and implications

This study reports the first complete time series of bloom development, N dynamics, and stable isotope composition of POM in early opening Arctic waters. The large difference in $\delta^{13}C_{org}$ between ice-grown material and water-column POM implies that pelagic biomass was produced in situ and, more generally, that seeding by ice algae is not necessary for early blooms to occur. Incidentally, the $\delta^{13}C_{org}$ of sediment organics should be a useful tracer of the relative importance of pelagic and ice-algal production to export/burial in Smith Sound and Baffin Bay. By ruling out the possibility

that ice algae jump-started the pelagic bloom in the North Water, we were able to ascribe changes in N uptake and PON inventory to pelagic processes and establish that the compensation irradiance of phytoplankton in the high Arctic is similar to the average for the North Atlantic. It follows that shallow mixing is instrumental to early pelagic growth in open waters of the Arctic Ocean.

The maintenance of shallow, mixed layers in the eastern North Water was associated with the stabilizing input of oceanic heat. Without it, the early attrition of ice promotes deep mixing and delays phytoplankton growth, as observed in the western North Water. When blooms are delayed until the onset of summer melt (e.g., the northwest North Water) it is difficult to tease apart the effect of light and seasonally increasing temperature on the course of a bloom. Our study demonstrated that precocious and rapid pelagic growth can be triggered long before the onset of seasonal warming in the high Arctic. Indeed, the N uptake capacity of diatoms rose by an order of magnitude despite constant, near-freezing temperatures in the eastern North Water. Although the increase in uptake capacity shortly followed exposure to high irradiance and was consistent with changes in the dark reactions of photosynthesis, the precise mechanism driving it requires further investigation.

Once the rate constraint imparted by the polar night and heavy snow/ice cover was relaxed, NO_3^- was entirely consumed in the mixed layer. Similar observations were made in other regions across the Arctic (e.g., Smith et al. 1997) despite differences in the timing of the productive period. Support for N limitation of biomass yield in the North Water was provided by the isotopic enrichment of PON and the near complete assimilation of N into POM.

In the Arctic Ocean, winter NO_3^- concentrations typically range from 12 μmol N L^{-1} in the Atlantic sector to as little as 2 μmol N L^{-1} in polar surface waters of the Beaufort Gyre. Although the nutrient-rich halocline underlying polar surface waters is considered resistant to vertical mixing, erosion events have been linked to synoptic storms (Yang et al. 2004), whose incidence and intensity are relatively high during positive phases of the Arctic oscillation (Zhang et al. 2004). In addition, upwelling-favorable winds along shelf breaks are conducive to nutrient replenishment under conditions of reduced ice cover (Carmack and Chapman 2003). In the North Water, vertical mixing contributed to episodic nutrient resupply in the east and to unusually high nutrient concentrations in the polar surface water entering the northwest (Tremblay et al. 2002*b*). The annual production supported by these nutrient subsidies far exceeds simple predictions based on the duration of the open water period (Rysgaard et al. 1999; Klein et al. 2002). Given the tight coupling between photosynthesis, NO_3^- consumption, and the *f*-ratio over the course of an early bloom, the magnitude of primary production and potential export should be considered highly responsive to climate and altered N supply in the changing Arctic Ocean.

References

ACIA. 2005. Scientific report: Arctic Climate Impact Assessment. Cambridge University Press.

ALLEN, A. E., M. H. HOWARD-JONES, M. G. BOOTH, M. E. FRISCHER, P. G. VERITY, D. A. BRONK, AND M. P. SANDERSON. 2002. Importance of heterotrophic bacterial assimilation of ammonium and nitrate in the Barents Sea during summer. J. Mar. Syst. **38:** 93–108.

AMINOT, A., AND R. KÉROUEL. 1982. Dosage automatique de l'urée dans l'eau de mer: une méthode très sensible à la diacetylmonoxime. Can. J. Fish. Aquat. Sci. **39:** 174–183.

ARRIGO, K. R., D. H. ROBINSON, R. B. DUNBAR, A. R. LEVENTER, AND M. P. LIZOTTE. 2003. Physical control of chlorophyll *a*, POC, and TPN distributions in the pack ice of the Ross Sea, Antarctica, J. Geophys. Res. **108.** [doi: 10.1029/2001JC001138]

———, ———, AND D. L. WORTHEN. 1999. Phytoplankton community structure and the drawdown of nutrients and CO_2 in the Southern Ocean. Science **283:** 365–367.

BOOTH, B. C., P. LAROUCHE, S. BÉLANGER, B. KLEIN, D. AMIEL, AND Z. P. MEI. 2002. Dynamics of *Chaetoceros socialis* blooms in the North Water. Deep-Sea Res. II **49:** 22–23.

BRANDES, J. A., AND A. H. DEVOL. 1997. Isotopic fractionation of oxygen and nitrogen in coastal marine sediments. Geochim. Cosmochim. Acta **61:** 1793–1801.

CARMACK, E., AND D. C. CHAPMAN. 2003. Wind-driven shelf/basin exchange on an Arctic shelf: The joint roles of ice cover extent and shelf-break bathymetry. Geophys. Res. Lett. **30.** [DOI: 10.1029/2003GL017526.]

COCHLAN, W. P., AND D. A. BRONK. 2001. Nitrogen uptake kinetics in the Ross Sea, Antarctica. Deep-Sea Res. II **48:** 19–20.

COLLOS, Y. 1987. Calculation of ^{15}N uptake rates by phytoplankton assimilating one or several nitrogen sources. Appl. Radiat. Isot. **38:** 275–282.

DICKEY, T., J. MARRA, D. E. SIGURDSON, R. A. WELLER, C. S. KINKADE, S. E. ZEDLER, J. D. WIGGERT, AND C. LANGDON. 2001. Seasonal variability of bio-optical and physical properties in the Arabian Sea: October 1994–October 1995. Deep-Sea Res. **45:** 10–11.

EPPLEY, R. W., AND B. J. PETERSON. 1979. Particulate organic matter flux and planktonic new production in the deep ocean. Nature **282:** 677–680.

FORTIER, M., L. FORTIER, C. MICHEL, AND L. LEGENDRE. 2002. Climatic and biological forcing of the vertical flux of biogenic particles under seasonal Arctic sea ice. Mar. Ecol. Prog. Ser. **225:** 1–16.

GANESHRAM, R. S., T. F. PEDERSEN, S. E. CALVERT, AND J. W. MURRAY. 1995. Large changes in oceanic nutrient inventories from glacial to interglacial periods. Nature **376:** 755–758.

GAO, Y., G. J. SMITH, AND R. S. ALBERTE. 2000. Temperature dependence of nitrate reductase activity in marine phytoplankton: Biochemical analysis and ecological implications. J. Phycol. **36:** 304–313.

GRASSHOFF, K. 1999. Methods of seawater analyses, 3rd ed. Weinheim.

HARRISON, W. G., AND T. PLATT. 1986. Photosynthesis-irradiance relationships in polar and temperate phytoplankton populations. Polar Biol. **5:** 153–164.

———, ———, AND B. IRWIN. 1982. Primary production and nutrient assimilation by natural phytoplankton populations of the eastern Canadian Arctic. Can. J. Fish. Aquat. Sci. **39:** 335–345.

HU, S., AND W. O. SMITH, JR. 1998. The effects of irradiance on nitrate uptake and dissolved organic nitrogen release by phytoplankton in the Ross Sea. Cont. Shelf Res. **18:** 971–990.

KASHINO, Y., S. KUDOH, Y. HAYASHI, Y. SUZUKI, T. ODATE, T. HIRAWAKE, K. SATOH, AND M. FUKUCHI. 2002. Strategies of phytoplankton to perform effective photosynthesis in the North Water. Deep-Sea Res. II **49:** 5049–5061.

KENNEDY, H., D. N. THOMAS, G. KATTNER, C. HAAS, AND G. S. DIECKMANN. 2002. Particulate organic matter in Antarctic summer sea ice: Concentration and stable isotopic composition. Mar. Ecol. Prog. Ser. **238:** 1–13.

KIRCHMAN, D. L., R. G. KEIL, AND P. A. WHEELER. 1989. The effect of amino acids on ammonium utilization and regeneration by heterotrophic bacteria in the subarctic Pacific. Deep-Sea Res. **36:** 1763–1776.

KLEIN, B., AND OTHERS. 2002. Phytoplankton biomass, production and potential export in the North Water. Deep-Sea Res. II **49:** 4983–5002.

KRISTIANSEN, S., AND T. FARBROT. 1991. Nitrogen uptake rates in phytoplankton and ice algae in the Barents Sea. Polar Res. **10:** 187–192.

———, ———, AND P. A. WHEELER. 1994. Nitrogen cycling in the Barents Sea—seasonal dynamics of new and regenerated production in the marginal ice zone. Limnol. Oceanogr. **39:** 1630–1642.

LAXON, S., N. PEACOCK, AND D. SMITH. 2003. High interannual variability of sea ice thickness in the Arctic region. Nature **425:** 947–950.

LOMAS, M. W., AND P. M. GLIBERT. 1999. Temperature regulation of nitrate uptake: A novel hypothesis about nitrate uptake and reduction in cool-water diatoms. Limnol. Oceanogr. **44:** 556–572.

LOVEJOY, C., L. LEGENDRE, M. J. MARTINEAU, J. BÂCLE, AND C. H. VON QUILLFELDT. 2002. Distribution of phytoplankton and other protists in the North Water. Deep-Sea Res. II **49:** 5027–5047.

MEI, Z. P., AND OTHERS. 2002. Physical control of spring-summer phytoplankton dynamics in the North Water, April–July 1998. Deep-Sea Res. II **49:** 4959–4982.

MELLING, H., Y. GRATTON, AND G. INGRAM. 2001. Ocean circulation within the North Water Polynya of Baffin Bay. Atmosph. Ocean **39:** 301–325.

MICHEL, C., M. GOSSELIN, AND C. NOZAIS. 2002. Preferential sinking export of biogenic silica during the spring and summer in the North Water Polynya (northern Baffin Bay): Temperature or biological control? J. Geophys. Res. **107.** [DOI: 10.1029/2000JC000408.]

———, L. LEGENDRE, R. G. INGRAM, M. GOSSELIN, AND M. LEVASSEUR. 1996. Carbon budget of sea-ice algae in spring: Evidence of a significant transfer to zooplankton grazers. J. Geophys. Res. **101:** 18345–18360.

MUGGLI, D. L., AND W. O. SMITH, JR. 1993. Regulation of nitrate and ammonium uptake in the Greenland Sea. Mar. Biol. **115:** 199–208.

NEEDOBA, J. A., AND P. J. HARRISON. 2004. Influence of low light and a light:dark cycle on NO_3^- uptake, intracellular NO_3^-, and nitrogen isotope fractionation by marine phytoplankton. J. Phycol. **40:** 505–516.

———, N. A. WASER, P. J. HARRISON, AND S. E. CALVERT. 2003. Nitrogen isotope fractionation in 12 species of marine phytoplankton during growth on nitrate. Mar. Ecol. Prog. Ser. **255:** 81–91.

NIEBAUER, H. J. 1991. Bio-physical oceanographic interactions at the edge of the Arctic ice pack. J. Mar. Syst. **2:** 209–232.

PRISCU, J. C. 1989. Photon dependence of inorganic nitrogen transport by phytoplankton in perennially ice-covered antarctic lakes. Hydrobiologia **172:** 173–182.

RICHARDSON, K., J. BEARDALL, AND J. A. RAVEN. 1983. Adaptation of unicellular algae to irradiance: An analysis of strategies. New Phytol. **93:** 157–191.

RYSGAARD, S., T. G. NIELSEN, AND B. W. HANSEN. 1999. Seasonal variation in nutrients, pelagic primary production and grazing in a high-Arctic coastal marine ecosystem, Young Sound, northeast Greenland. Mar. Ecol. Prog. Ser. **179:** 13–25.

SCHUBERT, C. J., AND S. E. CALVERT. 2001. Nitrogen and carbon isotopic composition of marine and terrestrial organic matter in Arctic Ocean sediments: Implications for nutrient utilization and organic matter composition. Deep-Sea Res. **48:** 789–810.

SIEGEL, D. A., S. C. DONEY, AND J. A. YODER. 2002. The North Atlantic spring phytoplankton bloom and Sverdrup's critical depth hypothesis. Science **296:** 730–733.

SIMARD, M. 2003. Influence des facteurs du milieu sur la dynamique printanière des microalgues de glace de la région des Eaux du Nord (baie de Baffin). M.Sc. thesis, Université du Québec à Rimouski, Canada.

SMETACEK, V., AND U. PASSOW. 1990. Spring bloom initiation and Sverdrup's critical-depth model. Limnol. Oceanogr. **35:** 228–234.

SMITH, W. O., JR., M. GOSSELIN, L. LEGENDRE, D. WALLACE, K. DALY, AND G. KATTNER. 1997. New production in the Northeast Water Polynya: 1993. J. Mar. Syst. **10:** 199–209.

———, L. A. CODISPOTI, D. M. NELSON, T. MANLEY, E. J. BUSKEY, H. J. NIEBAUER, AND G. F. COTA. 1991. Importance of *Phaeocystis* blooms in the high-latitude ocean carbon cycle. Nature **352:** 514–516.

———, AND W. G. HARRISON. 1991. New production in polar regions: The role of environmental controls. Deep-Sea Res. I **38:** 1463–1479.

STRASS, V. H., AND E. M. NÖTHIG. 1996. Seasonal shifts in ice edge phytoplankton blooms in the Barents Sea related to the water column stability. Polar Biol. **16:** 409–422.

TREMBLAY, J.-É., Y. GRATTON, E. C. CARMACK, C. D. PAYNE, AND N. M. PRICE. 2002*b*. Impact of the large-scale Arctic circulation and the North Water Polynya on nutrient inventories in Baffin Bay. J. Geophysis Res. **107.** [doi:10.1029/2000JC000595]

———, ———, J. FAUCHOT, AND N. M. PRICE. 2002*a*. Climatic and oceanic forcing of new, net, and diatom production in the North Water. Deep-Sea Res. II **49:** 4927–4946.

———, L. LEGENDRE, B. KLEIN, AND J. C. THERRIAULT. 2000. Size-differential uptake of nitrogen and carbon in a marginal sea (Gulf of St. Lawrence, Canada): Significance of diel periodicity and urea uptake. Deep-Sea Res. II **47:** 489–518.

———, AND W. O. SMITH, JR. In press. Primary production and nutrient dynamics in polynyas. *In* D. Barber and W. O. Smith, Jr. [eds.], Polynyas: Windows into polar oceans. Elsevier.

WU, J., S. E. CALVERT, AND C. S. WONG. 1997. Nitrogen isotope variations in the subarctic northeast Pacific: Relationships to nitrate utilization and trophic structure. Deep-Sea Res. I **47:** 287–314.

YANG, J., J. COMISO, D. WALSH, R. KRISHFIELD, AND S. HONJO. 2004. Storm-driven mixing and potential impact on the Arctic Ocean. J. Geophys. Res. **109.** [DOI: 10.1029/2001JC001248.]

ZHANG, X., J. E. WALSH, J. ZHANG, U.S. BHATT, AND M. IKEDA. 2004. Interannual variability of Arctic cyclone activity, 1948–2002. J. Clim. **17:** 2300–2317.

Received: 26 November 2004
Accepted: 21 July 2005
Amended: 3 October 2005